Measuring the Degeneracy of Discrete Energy Levels Using a GaAs/AlGaAs Quantum Dot

A. Hofmann,* V. F. Maisi, C. Gold, T. Krähenmann, C. Rössler, J. Basset, P. Märki, C. Reichl, W. Wegscheider, K. Ensslin, and T. Ihn
Solid State Physics Laboratory, ETH Zurich, CH-8093 Zurich, Switzerland
(Received 4 July 2016; published 11 November 2016)

We demonstrate an experimental method for measuring quantum state degeneracies in bound state energy spectra. The technique is based on the general principle of detailed balance and the ability to perform precise and efficient measurements of energy-dependent tunneling-in and -out rates from a reservoir. The method is realized using a GaAs/AlGaAs quantum dot allowing for the detection of time-resolved single-electron tunneling with a precision enhanced by a feedback control. It is thoroughly tested by tuning orbital and spin degeneracies with electric and magnetic fields. The technique also lends itself to studying the connection between the ground-state degeneracy and the lifetime of the excited states.

DOI: 10.1103/PhysRevLett.117.206803

Degeneracies play an important role in quantum statistics [1]. They often arise from symmetries of the underlying system [2,3] and govern the theoretical description of macroscopic quantum phenomena such as superconductivity [4] and the quantum Hall effect [5] but also play an important role for atomic spectra [6]. Theoretical concepts of topological protection are based on ground-state degeneracies [7], and modern schemes to control qubits make use of tunable degeneracies [8]. While the concept is omnipresent in quantum theory, measuring the degeneracy of an energy level in a quantum system seems to be less developed. A familiar way to experimentally demonstrate the existence of a degeneracy consists in breaking underlying symmetries, thereby lifting the degeneracy as in the Zeeman [9–12] or the Stark effect. Alternative techniques use selective excitations such as left- or right-circularly polarized light to distinguish degenerate excitations [13].

We demonstrate an experimental method of measuring the degeneracy of discrete energy levels alternative to the techniques mentioned above. The method is based on a general relation derived from detailed balance and makes use of tunneling spectroscopy and our ability to detect individual tunneling events in real time [14,15]. We overcome previous accuracy limitations of this technique [16] by implementing a feedback control. A single few-electron quantum dot in GaAs serves as the system of choice to test our experimental method. In this system, ground and excited states are well studied [9,17–25], and the presence of degeneracies is established from symmetry-breaking measurement techniques [9,11,17,20,21,26–30]. Our method reliably traces these degeneracies with great accuracy. Furthermore, the system combined with our measurement method allows us to controllably alter the degeneracy of energy levels. The method of degeneracy detection is very general and can be directly transferred to other systems where states are accessible by tunneling. For example, similar considerations have been used to study degeneracies in a time- and ensemble-averaged fashion in [31].

Our samples are made from a GaAs/AlGaAs heterostructure hosting a two-dimensional electron gas 90 nm below the surface. As shown in Fig. 1(a), we form a quantum dot by applying negative voltages to the metallic top-gate fingers, thereby depleting the electron gas below. The quantum dot is coupled by tunneling to an electron reservoir at a temperature of $T \approx 50$ mK. The presented measurements are performed on two different samples, in different cooldowns and cryostats.

At fixed gate voltages, single electrons tunnel back and forth between the dot and the reservoir if the addition energy μ_N for adding the Nth electron to the quantum dot is within the thermal energy window of approximately $3.5kT \approx 15$ μeV (k is the Boltzmann constant) around

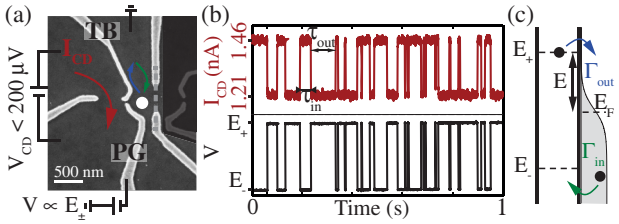

FIG. 1. Measurement setup. (a) The surface of the crystal with Ti/Au top gates in light gray and the two-dimensional electron gas underneath the dark area. An electron (white circle) tunnels back and forth between the quantum dot and the reservoir (blue and green arrows). The dotted line indicates a closed barrier, and biased gates are plotted in a brighter color than grounded gates. (b) The current (red arrow) through the charge detector as a function of time measures the occupation of the quantum dot [$(N-1) \approx 1.46$ nA, $N \approx 1.21$ nA]. The voltage, converted to energy, applied to the gate plunger gate (black) indicates the energies $E_{\pm}$ of the state μ_N, as indicated in the energy diagram of the quantum dot-reservoir system in (c).

the reservoir Fermi energy [32]. The addition energy μ_N is the energy difference between the N-electron and the $(N-1)$-electron many-body ground-state energies E_N and E_{N-1}, respectively, of the quantum dot. Each of these two energies can be degenerate, meaning that a number of microstates exist sharing the same N and E_N. The dot occupation changes through single-electron tunneling only between N and $N-1$, i.e., by only one electron, owing to the Coulomb blockade effect characterized by a charging energy of 1 meV $\gg kT$. In our experiment, we investigate small electron numbers $N < 9$.

We measure the quantum dot occupation with the current I_{CD} through a quantum point contact charge detector [see Fig. 1(a)] coupled capacitively to the dot [14,15]. Time-resolved traces of I_{CD} [see Fig. 1(b)] provide the statistically distributed waiting times τ_{in} for single-electron tunneling from the reservoir into the dot and τ_{out} for tunneling from the dot into the reservoir. An exponential speed-up compared to previous measurement schemes [14,30] allows us to measure these waiting times when μ_N is detuned from the Fermi energy E_F by much more than kT, where tunneling in one direction is exponentially suppressed due to the lack of occupied (empty) states in the reservoir for tunneling in (out). To speed up the measurement in the fast direction, we implement a feedback mechanism to switch the level cyclically between $E_\pm = E_F \pm E$ [see Figs. 1(b) and 1(c)]. The waiting time for an electron to tunnel out at $\mu_N = E_F + E$ gives an instance of $\tau_{\mathrm{out}}(E)$. After the detection of the tunneling-out event, we quickly switch the empty level to $\mu_N = E_F - E$, where we wait for an electron to tunnel in, thereby measuring an instance of $\tau_{\mathrm{in}}(-E)$. The occupied level is switched back to $E_F + E$, where the cycle restarts. An electronic feedback triggers the voltage switch between $E_\pm$ when the respective change in occupation has been detected. Tunneling rates $\Gamma_{\mathrm{out/in}}(\pm E) = \langle \tau_{\mathrm{out/in}}(\pm E) \rangle^{-1}$ are obtained by averaging the waiting times over time traces of 10 s.

Measurements of $\Gamma_{\mathrm{out/in}}(E)$ are shown in Fig. 2 for tunneling resonances corresponding to filling the first eight electrons into the quantum dot. We observe that tunneling-in rates (green) are essentially constant for energies below resonance, usually with a weak linear energy dependence superimposed [33]. Above resonance, these rates are exponentially suppressed according to the Fermi-distribution function. Conversely, tunneling-out rates (blue) are essentially constant for energies above resonance (with a weak linear energy dependence superimposed) and decrease exponentially for energies below. All measured curves in Fig. 2 agree with

$$\Gamma_{\mathrm{in}}(E) = W_{\mathrm{in}}(E) f(E),$$
$$\Gamma_{\mathrm{out}}(E) = W_{\mathrm{out}}(E)[1 - f(E)], \qquad (1)$$

with the Fermi-distribution function $f(E)$ and the energy-dependent tunnel couplings $W_{\mathrm{in/out}}(E)$. Fitting the measured tunneling-in and -out rates to Eqs. (1) with the functions $W_{\mathrm{in/out}}(E) = W_{0,\mathrm{in/out}}(1 + \alpha E)$ and the fitting parameters $W_{0,\mathrm{in/out}}$ and α, we determine the ratios of tunneling rates on resonance $W_{0,\mathrm{in}}/W_{0,\mathrm{out}}$. For the first eight resonances of the quantum dot, they alternate between integer ratios 2:1 and 1:2, as indicated in Fig. 2.

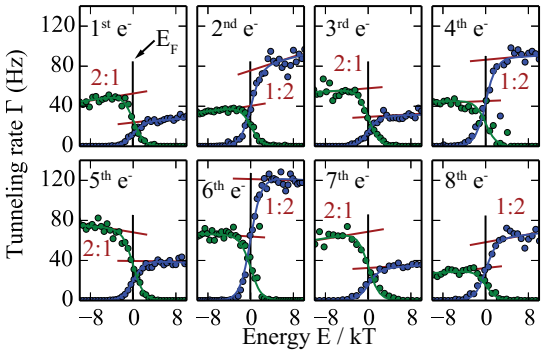

FIG. 2. Tunneling rates of the first eight resonances around the reservoir Fermi energy (zero energy reference). Green and blue denote the tunneling-in and tunneling-out rate, respectively. The solid lines are fits to Eq. (1), and the red lines are guides to the eye indicating the ratio $W_{0,\mathrm{in}} : W_{0,\mathrm{out}}$ of the tunnel couplings to alternate between 2:1 and 1:2.

This result may seem surprising in the light of the time-reversal symmetry of tunneling. In this view, $W_{0,\mathrm{in}} = W_{0,\mathrm{out}}$ is expected, as the tunnel coupling of a given quantum dot state to the reservoir does not depend on the direction of tunneling. However, this reasoning is incomplete, because it neglects possible degeneracies of the initial and final quantum dot states involved in the tunneling event [16,33]. One finds on the basis of detailed balance that

$$\frac{W_{0,\mathrm{in}}}{W_{0,\mathrm{out}}} = \frac{p_N}{p_{N-1}} = \frac{m}{n}, \qquad (2)$$

where m is the degeneracy of the N-electron and n that of the $(N-1)$-electron energy level and p_N and p_{N-1} are the time-averaged occupation probabilities of the two levels. Equation (2) is the basic relation that allows us to determine the degeneracies of the different E_N from the measurements in Fig. 2. It is likely that different orbitally degenerate states have different tunnel couplings. Nevertheless, Eq. (2) is a ratio of integers, given only by the degeneracy of the initial and final states. For weak energy dependence α, this ratio can be read directly from the saturation values of the tunneling rates at high and low energies.

For example, the resonance for filling the first electron in Fig. 2 is a transition between the singly occupied dot $(N = 1)$ and the empty dot $(N - 1 = 0)$, which has a nondegenerate energy $E_0 = 0$ leading to $n = 1$. The measured ratio $W_{0,\mathrm{in}} : W_{0,\mathrm{out}} = m : n = 2 : 1$ indicates a twofold degenerate $(m = 2)$ level E_1. It is well known for this system that indeed the E_1 state has a twofold spin degeneracy [34]. The resonance for filling the second electron is a transition between the twofold degenerate

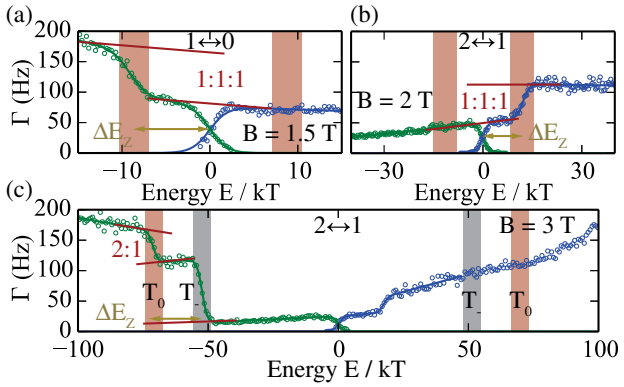

FIG. 3. Tunneling rates at a finite magnetic field for the first (a) and second (b) resonance. The Zeeman energy is $\Delta E_Z = g\mu_B B = |E_{es}|$ with the g factor $|g| = 0.44$ and the Bohr magneton μ_B. The solid blue and green lines are fits to a modification of Eq. (1) with adding energetically offset tunneling rates. The red lines are guides to the eye and indicate the ratios 1:1:1 for tunneling into the ground state, tunneling into the Zeeman-split excited state and tunneling out of the ground state. The ratios for the first and second electron are $W_{0,\mathrm{out}}:W_{0,\mathrm{in}}:W^{Z}_{0,\mathrm{in}} = 76.7:78.5:75.4$ and $W_{0,\mathrm{out}}:W_{0,\mathrm{in}}:W^{Z}_{0,\mathrm{in}} = 49.9:54.7:59.1$, respectively. (c) Excited state spectroscopy of the second electron. The solid lines are fits to Eq. (1) with three (two) energetically offset tunneling-in (-out) rates. The red lines indicate the ratio 2:1 for tunneling into the triplet states T_- and T_0, $W^{T_-}_{0,\mathrm{in}}:W^{T_0}_{0,\mathrm{in}} = 105:54$.

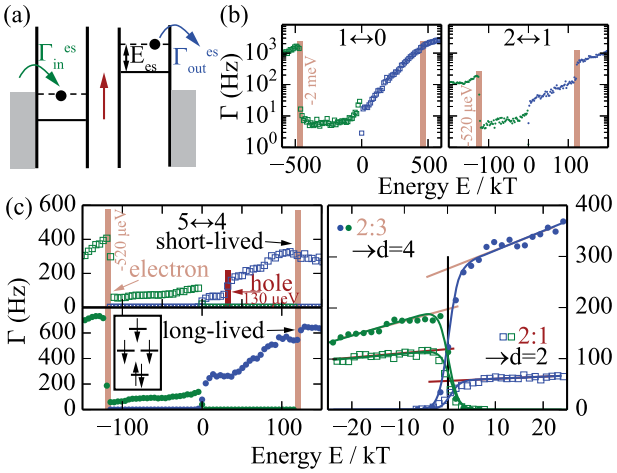

FIG. 4. Excited state spectroscopy ($kT \approx 3.4$ μeV), showing that the feedback technique allows us to infer degeneracy, excitation spectrum, and spin states from one quick measurement. The quantum dot states are driven symmetrically as shown in (a) to measure the tunneling rates Γ_{in} and Γ_{out}. The data are plotted as open squares (closed circles) in (b) for the one-electron (two-electron) state being driven around the Fermi energy. N-electron excitations are indicated with red bars and show a short-lived excitation (no step) for the $N = 1$ state and long-lived excitation (step visible) for the $N = 2$ state. The spectroscopy around $\mu_{N=5}$ is shown in (c) for the spin-degenerate (top-left panel, $d = 2$) and the orbital degenerate (bottom-left panel, $d = 4$) ground state in open squares and closed circles, respectively. The right panel shows an enlargement around zero energy with the tunnel barrier being slightly more open.

E_1 state ($n = 2$) and the E_2 state. The measured ratio of $W_{0,\mathrm{in}}:W_{0,\mathrm{out}} = m:n = 1:2$ indicates a nondegenerate level E_2. This agrees with the well-known nondegenerate spin-singlet ground state of the two-electron dot [9,12,26,34,35], where two electrons with opposite spin occupy the lowest orbital single-particle state. Along these lines, we interpret the series of results in Fig. 2 as a sequence of alternating spin-up and spin-down filling into the quantum dot, where energy levels E_N are spin degenerate for odd N and nondegenerate for even N up to $N = 8$. This result fits well to the expectations in an asymmetric confinement potential with orbitally nondegenerate single-particle states [36].

To further test the applicability of Eq. (2), we use an in-plane magnetic field to lift the spin degeneracy of the one-electron ground state by the Zeeman effect. The result is shown in Fig. 3(a) for the tunneling transitions between the empty and the one-electron dot and in Fig. 3(b) for the transition between the one- and two-electron ground state. The ratio of the ground-state transition rates now changed to $W_{0,\mathrm{in}}:W_{0,\mathrm{out}} = 1:1$ in both cases as predicted by Eq. (2) for nondegenerate zero-, one-, and two-electron ground states.

The feedback technique also gives access to excitations far above the ground-state energies on the scale of kT. Excited states of the N-electron system can be accessed [33,37–39], when the dot is initially in the $(N-1)$-electron ground state, and the tunneling-in process takes the system into an N-electron excited state [see the schematic in Fig. 4(a)]. An example of such a process is shown in Fig. 3(a), where a thermally broadened step is seen in the tunneling-in rate into the empty dot (green) close to $E = -9kT \approx -\Delta E_Z$, the Zeeman energy, due to the additional tunneling-in channel provided by the spin excitation. A pronounced step is observed in the tunneling-out rate at ΔE_Z in Fig. 3(b) due to the same spin excitation of the one-electron dot, in which the dot remains after the tunneling-out event.

The analysis of the excited states gives more insight into the tunnel coupling of the different states to the lead. We fit the tunneling-in rate in Fig. 3(a) to $[W_{0,\mathrm{in}}f(E) + W_{0,\mathrm{es}}f(E - E_{\mathrm{es}})][1 - \alpha E]$ and find $W_{0,\mathrm{in}} = W_{0,\mathrm{es}} = 1:1$. Analyzing the same excited state in Fig. 3(b), we find the same ratio for the tunneling-out rates. This result agrees with the notion that the orbital single-particle wave functions of the two spin states are the same. This precise [relative error $< 14\%$ in Fig. 3(a)] experimental validation of equal tunneling rates is important for charge-to-spin conversion by spin-selective readout of the charge state [37,39–41].

The spin-triplet excitations of the two-electron state provide the possibility to compare their tunnel rates quantitatively. In Fig. 3(c), we observe two excitations in the transition between $(N-1) = 1$ and $N = 2$,

corresponding to the triplet states T_0 and T_-, where the tunnel rate of the T_- state is twice as large as that of the T_0 state. The T_+ excited state is not observed. These observations are entirely due to the overlap of the spin parts of initial and final states. The initial state is a statistical mixture of the one-electron quantum dot ground state with spin parallel to the magnetic field and any spin orientation in the reservoir, i.e., of $|\downarrow\rangle \otimes |\downarrow\rangle$ and $|\downarrow\rangle \otimes |\uparrow\rangle$. Its overlap with the final T_+ state $|\uparrow\uparrow\rangle$ where both spins in the dot are antiparallel to the field is therefore zero, and the T_+ excited state is not observed [12,42,43]. In contrast, the T_0 final state is $(|\uparrow\downarrow\rangle + |\downarrow\uparrow\rangle)/\sqrt{2}$, giving a factor of $1/2$ in the squared overlap between initial and final states as compared to the T_- state $|\downarrow\downarrow\rangle$.

At zero magnetic field, we perform spectroscopy of the orbital states utilizing the feedback technique. Figure 4(b) shows an excited state measurement, where an excitation of the two-electron (one-electron) dot is filled at $-120kT(-460kT) \approx -520$ μeV (-2 meV), as seen in the tunneling-in rate (green). Interestingly, a corresponding step appears at $+120kT$ in the tunneling-out rate (blue) in the two-electron case. Obviously, the two-electron dot remains in the excited state for a longer time than the feedback needs to switch the system to higher energy, which is 1.2 ms in our experiment. Tunneling out from this excited state contributes to the tunneling-out rate at higher energies [see Fig. 4(a)]. This attests to the long relaxation time of this lowest excitation, which is known to be the spin-triplet state above the spin-singlet ground state [38,39] requiring a hyperfine-interaction- or spin-orbit-interaction-mediated spin flip [44,45] for relaxing to the spin-singlet ground state [34,46–48]. A similar mirror step was not seen for the excited state in the left panel in Fig. 4(b), because orbital excitations have lifetimes shorter by many orders of magnitude than those of spin excitations [34,48]. This example illustrates the remarkable ability [34,49] of the excited state measurement scheme to distinguish spin excitations from orbital excitations, at zero magnetic field.

We observe a variant of the excited state spectroscopy for the tunneling transition between the four- and the five-electron quantum dot shown in the top panel in Fig. 4(c). In addition to the fast decaying (purely orbital) excitation of the five-electron state visible in the tunneling-in rate (green) at $-120kT \approx 520$ μeV, a pronounced step is observed in the tunneling-out rate at $+30kT \approx 130$ μeV. We interpret this step as an excitation of the four-electron $(N-1)$ dot, in which the dot remains after the tunneling-out event, and therefore label it "hole." An anisotropic two-dimensional harmonic oscillator [50–52] has a single-particle spectrum with two excited state orbitals close in energy but far above the single-particle ground-state orbital. It is plausible that, in our quantum dot, two electrons occupy the lowest orbital and that the observed orbital excitation of the four-electron system is a single-particle excitation into the higher lying of the nearly-degenerate orbitals.

Next, we turn our attention to the degeneracy measurement of orbitally degenerate states, which in general have different tunnel coupling constants. The orbital excitation of the four-electron system is tuned into resonance with the ground state by a suitable change in gate voltages [24]. The tunneling rates measured in this situation are shown in the lower panel in Fig. 4(c), where the five-electron excitation is still seen in the tunneling-in rate, but the four-electron excitation is resonant with the four-electron ground state, giving a nontrivial further testing ground for the application of Eq. (2). The enlargement in the right panel in Fig. 4(c) shows that the ratio of tunneling rates $W_{0,\mathrm{in}}:W_{0,\mathrm{out}}$ has changed from $2:1$ (open squares; cf. Fig. 2) to $2:3$ (solid circles).

The $2:3$ ratio of degeneracies of the five- and four-electron quantum dot is understood within the picture of the single-particle orbital states of the anisotropic two-dimensional harmonic oscillator [52]. The single-particle orbital lowest in energy takes two electrons. If the next higher orbital energy is twofold degenerate (hence fourfold degenerate in total due to the spin degeneracy of each orbital), the three-electron system has a degeneracy of four, the four-electron system of six, and the five-electron system of four. These numbers are obtained from counting the number of ways electrons can be distributed onto the four degenerate single-particle states. According to Eq. (2), this scenario indeed accounts for the observed ratio $2:3 = 4:6$ for the tunneling transition between the four- and the five-electron dots. Equation (2) is valid also for degenerate states with different tunnel coupling, because it is derived only from detailed balance and the second law of thermodynamics.

The lifetime of the five-electron quantum dot excitation seen at $-120kT$ in the top left panel in Fig. 4(d) is short compared to our switching time, if the four-electron ground state is twofold spin degenerate. After tuning this degeneracy to four, the lifetime of the five-electron excitation has increased as witnessed by the mirror step at $+120kT$ in the lower panel in the same figure. We conclude from the long lifetime that at least one relaxation channel requires a spin flip [inset in Fig. 4(d)], which means that the four-electron ground state is a spin-triplet state (Hund's rules). This demonstrates the connection between ground-state degeneracy and the excitation lifetime and agrees with measurements where parallel spin alignment of the four-electron ground state has been observed in circular [17,53,54] but not in elliptical dots [10,55].

In conclusion, we demonstrated ways to precisely measure and tune the degeneracy of a quantum state, by accessing its tunneling rates in a large energy window. We showed how a quick measurement of the tunneling rates simultaneously provides information about the degeneracy and spin configuration. It will be interesting to measure the magnetic field dependence of the lifetimes of excited states and, in particular, to study the lifetime of the T_0 state in comparison to the lifetime of the T_- state. Additionally, the

feedback loop can be operated in the reverse direction and thereby realize, for example, a Maxwell demon setting, which enables cooling of the reservoir using information.

We thank Mark Eriksson for stimulating discussions. We acknowledge the NCCR QSIT via the SNF, and ETH Zürich for providing the funding which enabled this work.

*andrea.hofmann@phys.ethz.ch

[1] K. Huang, *Statistical Mechanics*, 2nd ed. (Wiley-VCH, Berlin, 1988).
[2] E. Noether, Transp. Theory Stat. Phys. **1**, 186 (1971).
[3] M. El-Batanouny and F. Wooten, *Symmetry and Condensed Matter Physics* (Cambridge University Press, Cambridge, 2008).
[4] W. Buckel and R. Kleiner, *Superconductivity: Fundamentals and Applications*, 2nd ed. (Wiley-VCH, Berlin, 2004).
[5] *The Quantum Hall Effect*, 2nd ed., edited by R. E. Prange and S. M. Girvin (Springer-Verlag, New York, 1990).
[6] L. Landau and E. Lifshitz, *Course of Theoretical Physics*, 3rd ed. (Butterworth-Heinemann, London, 1981), Vol. 3.
[7] M. Freedman, A. Kitaev, M. Larsen, and Z. Wang, Bull. Am. Math. Soc. **40**, 31 (2003).
[8] M. A. Nielsen and I. L. Chuang, *Quantum Computation and Quantum Information* (Cambridge University Press, Cambridge, 2010).
[9] S. Tarucha, D. G. Austing, T. Honda, R. J. van der Hage, and L. P. Kouwenhoven, Phys. Rev. Lett. **77**, 3613 (1996).
[10] S. Sasaki, D. G. Austing, and S. Tarucha, Physica (Amsterdam) **256–258B**, 157 (1998).
[11] S. Lindemann, T. Ihn, T. Heinzel, W. Zwerger, K. Ensslin, K. Maranowski, and A. C. Gossard, Phys. Rev. B **66**, 195314 (2002).
[12] R. Hanson, L. M. K. Vandersypen, L. H. Willems van Beveren, J. M. Elzerman, I. T. Vink, and L. P. Kouwenhoven, Phys. Rev. B **70**, 241304 (2004).
[13] M. I. Miah and L. Naheed, Opt. Quantum Electron. **47**, 1239 (2015).
[14] R. Schleser, E. Ruh, T. Ihn, K. Ensslin, D. C. Driscoll, and A. C. Gossard, Appl. Phys. Lett. **85**, 2005 (2004).
[15] L. M. K. Vandersypen, J. M. Elzerman, R. N. Schouten, L. H. W. v. Beveren, R. Hanson, and L. P. Kouwenhoven, Appl. Phys. Lett. **85**, 4394 (2004).
[16] S. Gustavsson, R. Leturcq, M. Studer, I. Shorubalko, T. Ihn, K. Ensslin, D. C. Driscoll, and A. C. Gossard, Surf. Sci. Rep. **64**, 191 (2009).
[17] L. P. Kouwenhoven, T. H. Oosterkamp, M. W. S. Danoesastro, M. Eto, D. G. Austing, T. Honda, and S. Tarucha, Science **278**, 1788 (1997).
[18] J. Cooper, C. G. Smith, D. A. Ritchie, E. H. Linfield, Y. Jin, and H. Launois, Physica (Amsterdam) E **6**, 457 (2000).
[19] C. Gould, P. Hawrylak, A. Sachrajda, Y. Feng, P. Zawadzki, and Z. Wasilewski, Physica (Amsterdam) E **6**, 461 (2000).
[20] M. Ciorga, A. S. Sachrajda, P. Hawrylak, C. Gould, P. Zawadzki, S. Jullian, Y. Feng, and Z. Wasilewski, Phys. Rev. B **61**, R16315 (2000).
[21] R. M. Potok, J. A. Folk, C. M. Marcus, V. Umansky, M. Hanson, and A. C. Gossard, Phys. Rev. Lett. **91**, 016802 (2003).
[22] S. Sasaki, T. Fujisawa, T. Hayashi, and Y. Hirayama, Phys. Rev. Lett. **95**, 056803 (2005).
[23] T. Meunier, I. T. Vink, L. H. Willems van Beveren, K.-J. Tielrooij, R. Hanson, F. H. L. Koppens, H. P. Tranitz, W. Wegscheider, L. P. Kouwenhoven, and L. M. K. Vandersypen, Phys. Rev. Lett. **98**, 126601 (2007).
[24] S. Amasha, K. MacLean, I. P. Radu, D. M. Zumbühl, M. A. Kastner, M. P. Hanson, and A. C. Gossard, Phys. Rev. Lett. **100**, 046803 (2008).
[25] M. Xiao, M. G. House, and H. W. Jiang, Phys. Rev. Lett. **104**, 096801 (2010).
[26] R. C. Ashoori, H. L. Stormer, J. S. Weiner, L. N. Pfeiffer, K. W. Baldwin, and K. W. West, Phys. Rev. Lett. **71**, 613 (1993).
[27] J. A. Folk, J. A. Folk, C. M. Marcus, R. Berkovits, R. Berkovits, R. Berkovits, I. L. Kurland, I. L. Aleiner, B. L. Altshuler, and B. L. Altshuler, Phys. Scr. **T90**, 26 (2001).
[28] S. Lüscher, T. Heinzel, K. Ensslin, W. Wegscheider, and M. Bichler, Phys. Status Solidi (b) **224**, 561 (2001).
[29] S. Lüscher, T. Heinzel, K. Ensslin, W. Wegscheider, and M. Bichler, Phys. Rev. Lett. **86**, 2118 (2001).
[30] S. Hellmüller, D. Bischoff, T. Müller, M. Beck, K. Ensslin, and T. Ihn, Phys. Rev. B **92**, 115401 (2015).
[31] A. Beckel, A. Kurzmann, M. Geller, A. Ludwig, A. D. Wieck, J. König, and A. Lorke, Europhys. Lett. **106**, 47002 (2014).
[32] T. Ihn, *Semiconductor Nanostructures: Quantum States and Electronic Transport* (Cambridge University Press, Cambridge, 2009).
[33] K. MacLean, S. Amasha, I. P. Radu, D. M. Zumbühl, M. A. Kastner, M. P. Hanson, and A. C. Gossard, Phys. Rev. Lett. **98**, 036802 (2007).
[34] T. Fujisawa, D. G. Austing, Y. Tokura, Y. Hirayama, and S. Tarucha, Nature (London) **419**, 278 (2002).
[35] R. Hanson, L. P. Kouwenhoven, J. R. Petta, S. Tarucha, and L. M. K. Vandersypen, Rev. Mod. Phys. **79**, 1217 (2007).
[36] T. Ezaki, N. Mori, and C. Hamaguchi, Phys. Rev. B **56**, 6428 (1997).
[37] J. M. Elzerman, R. Hanson, L. H. Willems van Beveren, B. Witkamp, L. M. K. Vandersypen, and L. P. Kouwenhoven, Nature (London) **430**, 431 (2004).
[38] R. Hanson, L. H. Willems van Beveren, I. T. Vink, J. M. Elzerman, W. J. M. Naber, F. H. L. Koppens, L. P. Kouwenhoven, and L. M. K. Vandersypen, Phys. Rev. Lett. **94**, 196802 (2005).
[39] S. Amasha, K. MacLean, I. P. Radu, D. M. Zumbühl, M. A. Kastner, M. P. Hanson, and A. C. Gossard, Phys. Rev. B **78**, 041306 (2008).
[40] K. C. Nowack, M. Shafiei, M. Laforest, G. E. D. K. Prawiroatmodjo, L. R. Schreiber, C. Reichl, W. Wegscheider, and L. M. K. Vandersypen, Science **333**, 1269 (2011).
[41] C. B. Simmons, J. R. Prance, B. J. Van Bael, T. S. Koh, Z. Shi, D. E. Savage, M. G. Lagally, R. Joynt, M. Friesen, S. N. Coppersmith, and M. A. Eriksson, Phys. Rev. Lett. **106**, 156804 (2011).
[42] R. Hanson, I. T. Vink, D. P. DiVincenzo, L. M. K. Vandersypen, J. M. Elzerman, L. H. W. van Beveren, and L. P. Kouwenhoven, arXiv:cond-mat/0407793.

[43] J. M. Elzerman, R. Hanson, L. H. W. v. Beveren, L. M. K. Vandersypen, and L. P. Kouwenhoven, Appl. Phys. Lett. **84**, 4617 (2004).
[44] T. Fujita, P. Stano, G. Allison, K. Morimoto, Y. Sato, M. Larsson, J.-H. Park, A. Ludwig, A. D. Wieck, A. Oiwa, and S. Tarucha, preceding Letter, Phys. Rev. Lett. **117**, 206802 (2016).
[45] V. F. Maisi, A. Hofmann, M. Röösli, J. Basset, C. Reichl, W. Wegscheider, T. Ihn, and K. Ensslin, Phys. Rev. Lett. **116**, 136803 (2016).
[46] H. O. Li, M. Xiao, G. Cao, J. You, and G. P. Guo, Physica (Amsterdam) E **56**, 1 (2014).
[47] W. A. Coish, V. N. Golovach, J. C. Egues, and D. Loss, Phys. Status Solidi (b) **243**, 3658 (2006).
[48] A. V. Khaetskii and Y. V. Nazarov, Phys. Rev. B **61**, 12639 (2000).
[49] L. H. W. v. Beveren, R. Hanson, I. T. Vink, F. H. L. Koppens, L. P. Kouwenhoven, and L. M. K. Vandersypen, New J. Phys. **7**, 182 (2005).
[50] V. Fock, Z. Phys. **47**, 446 (1928).
[51] C. G. Darwin, Math. Proc. Cambridge Philos. Soc. **27**, 86 (1931).
[52] B. Schuh, J. Phys. A **18**, 803 (1985).
[53] C. Ellenberger, T. Ihn, C. Yannouleas, U. Landman, K. Ensslin, D. Driscoll, and A. C. Gossard, Phys. Rev. Lett. **96**, 126806 (2006).
[54] M. Koskinen, M. Manninen, and S. M. Reimann, Phys. Rev. Lett. **79**, 1389 (1997).
[55] D. G. Austing, S. Sasaki, S. Tarucha, S. M. Reimann, M. Koskinen, and M. Manninen, Phys. Rev. B **60**, 11514 (1999).